Sustainable Energy & Fuels

ROYAL SOCIETY OF CHEMISTRY

PAPER

View Article Online
View Journal

Cite this: DOI: 10.1039/d2se00399f

Hydrotreating of bio-crude obtained from hydrothermal liquefaction of biopulp: effects of aqueous phase recirculation on the hydrotreated oil†

Komeil Kohansal,[a] Kamaldeep Sharma,[a] Muhammad Salman Haider,[a] Saqib Sohail Toor,[a] Daniele Castello,[a] Lasse Aistrup Rosendahl,[a] Joscha Zimmermann[b] and Thomas Helmer Pedersen *[a]

Aqueous phase recirculation (APR) during the hydrothermal liquefaction (HTL) process is a means to enhance HTL performance and lower the need for intensive residual water treatment. However, the obtained HTL bio-crude cannot be considered a drop-in biofuel partially due to its significant heteroatom content. Thus, catalytic hydrotreating is typically practised to upgrade HTL bio-crude to drop-in biofuel/biofuel precursors. This study establishes a holistic overview of the influence of APR on hydrotreated bio-crude. The employed strategy integrates a four-step APR process to a batch catalytic hydrotreating process operating at mild (350 °C) or severe conditions (400 °C). APR revealed promising results in terms of bio-crude yield and energy recovery. However, the heteroatom content of the resulting bio-crude was noticeably elevated. Regardless of the operational conditions, hydrotreating experiments disclosed a higher oil yield while treating the first cycle's bio-crude along with limited coke formation. Although the added oxygen content by APR was offset through hydrotreating, the nitrogen content of the hydrotreated bio-crude in the consecutive cycles significantly increased. The elemental distribution results revealed that APR increased the nitrogen distribution in the hydrotreated bio-crude. Hence, higher quantities of hydrogen and severe hydrotreating conditions were required to obtain a suitable drop-in quality of the biofuel.

Received 22nd March 2022
Accepted 6th May 2022

DOI: 10.1039/d2se00399f

rsc.li/sustainable-energy

1. Introduction

In recent decades, the unrestrained consumption of fossil resources has raised enormous environmental challenges such as pronounced sulphur, nitrogen oxide, and carbon dioxide emissions into the atmosphere. Commencing from the early 20th century and with eminent concerns toward energy security, the scientific community and policy-makers have been pushed to pursue sustainable energy and fuels due to their potential benefits of being carbon-neutral and environmentally-friendly. Among various established eco-friendly technologies and their inherent pros/cons, increasingly significant attention has been drawn to hydrothermal liquefaction (HTL), a technology capable of processing wet/dry biomass and thereby eliminating the cost-prohibitive pre-drying step.[1] HTL efficiently produces a liquid energy carrier (namely bio-crude) with relatively low oxygen and high heating value (up to 90% of petroleum heating value).[2] However, depending on feedstock and the operational conditions, HTL produces a substantial quantity of water-miscible organics as a byproduct.[3] The carbon-rich aqueous phase causes process energy loss and requires an intensive subsequent wastewater treatment, contributing to above 90% of total waste disposal expenses.[4] As a result, valorizing the aqueous effluent to facilitate the commercial-scale implementation of HTL is currently an extensively explored topic.

Depending on the initial feedstock, the aqueous phase stream contains a significant quantity of organic compounds with high heteroatom content as well as inorganic nutrients. Therefore, many researchers investigated various biological and physiological aqueous phase management methods such as recycling through microbial and microalgae cultivation, catalytic hydrothermal gasification, and anaerobic digestion.[5–7] Recently, direct aqueous phase recirculation (APR) in the HTL process, by which the intensity of a required residual water post-treatment process can be considerably diminished, has been suggested by many studies.[8,9] Despite the economical-feasibility challenges for highly moist feedstocks, APR retains a higher

[a]AAU Energy, Aalborg University, Pontoppidanstræde 111, 9220 Aalborg Øst, Denmark. E-mail: thp@et.aau.dk

[b]Institute of Catalysis Research and Technology (IKFT), Karlsruhe Institute of Technology (KIT), Hermann-von-Helmholtz-Platz 1, 76344 Eggenstein-Leopoldshafen, Germany

† Electronic supplementary information (ESI) available. See https://doi.org/10.1039/d2se00399f

value to the process by enhancing the ultimate bio-crude production and/or energy recovery (ER). Chen *et al.* reported a significant increment of the bio-crude (12.7 wt%) and bio-char (2.6 wt%) yield after five consecutive cycles while hydrothermally treating *Chlorella* sp.[10] Shah *et al.* investigated the HTL of bio-digested sewage sludge upon consecutive APR. After five recirculation cycles, the bio-crude revealed significantly higher energy recovery (64.30%) compared to that of the reference experiment (38.83%).[11] Chen *et al.* investigated the effect of APR in HTL of *Spirulina platensis*, α-cellulose, and lignin. Thereby, bio-crude production and energy recovery in the case of *Spirulina platensis* were respectively increased by 9.7 wt% and 8.46%.[12] A plethora of literature highlights the effectiveness of APR in producing higher quantities of bio-crude, while the potential drawbacks have rarely been discussed.[3] Furthermore, due to the complexity and unsuitable chemical and physicochemical properties of the produced bio-crude, tremendous refinement before converting it to marketable fuels is required.

Catalytic hydrotreating (HT) of the bio-crude has received remarkable attention as a technology by which organic contaminants can be removed, and aromatics and olefins are hydrogenated to a great extent, leading to a higher quality of the hydrotreated oil.[13] Haider *et al.* carried out a Ni–Mo/γ-Al_2O_3-assisted parametric study on the hydrotreatment of *Spirulina* microalgae bio-crude. The temperature was concluded to be the most influential parameter on deoxygenation (de-O). However, the interaction of operating pressure and temperature had a key influence on denitrogenation (de-N).[14] Castello *et al.* studied the effect of initial H_2 pressure (4 and 8 MPa) on hydrotreatment of three different bio-crude feedstocks at 350 and 400 °C. It was highlighted that regardless of the feedstock, de-N required harsher operating conditions, *i.e.* higher temperature (400 °C) and high initial H_2 pressure.[15] Biller *et al.* investigated the performance of commercial catalysts in the hydrotreating of *Chlorella* microalgae bio-crude at mild (350 °C) and harsh (405 °C) temperature conditions. At higher temperature, the oxygen content of the bio-crude was reduced by 85% along with 60% of the nitrogen removal, revealing the resistance of some nitrogen compounds toward typical hydrotreating conditions.[16] Haider *et al.* also explored a two-stage hydrotreating strategy to overcome the thermal instability of HTL bio-crude under severe conditions (400 °C) required for successful denitrogenation. They observed that complete de-O was already achieved in the first stage (operating at the mild condition), while less than 60% of nitrogen was removed. Proceeding to the second stage and with the expense of higher H_2 consumption, de-N increased up to 92%.[17] High nitrogen content and denitrogenation of the bio-crude stand out as serious technical challenges in downstream processes due to strict fuel specification standards. Moreover, many researchers have reported the poisonous effect of different N-containing compounds on the refinery catalysts.[18,19] On the other hand, few previous studies have concluded that APR can potentially increase the nitrogen and heavy metal contents of ultimate HTL bio-crude, whereas there is limited information regarding the impact of different nitrogen species (originated or promoted by APR) on a downstream process in the literature.[9,20] In this regard, a detailed investigation of the mutual interaction of catalytic hydrotreating and heteroatomic compounds of bio-crude before and after APR is highly demanded.

The presented study firstly explores sequential concentrated APR while treating wet biomass. The evolution of bio-crude yield, chemical, and thermochemical properties are deeply investigated while employing a lab-scale batch HTL reactor with low cooling and heating rates. The impact of reactor type compared to our previous study is briefly discussed in terms of bio-crude yield and quality. Secondly, the study investigates the role of APR on the product distribution and heteroatom content of the hydrotreated oil by adopting a set of catalytic hydrotreating of the reference bio-crude (obtained without APR) and the consecutive bio-crude sample. The integrated carbon and nitrogen distribution throughout the entire process (HTL/HT) is demonstrated to answer the question 'is higher always better?'. Lately, the major nitrogen species presented in different oil samples are quantified to highlight the impact of APR on the chemical composition of the hydrotreated oils.

2. Materials and methods

2.1. Materials

The biomass used in this study is the organic fraction of municipal solid waste (biopulp), pretreated by Gemidan Ecogi A/S (Hjallerup, Denmark).[21] Tables S1† present the chemical, biochemical, and thermochemical properties of biopulp. Moreover, the inorganic content of the biopulp and the utilized analysis techniques are represented in our previous study.[22] The pre-sulfided commercial Ni–Mo/Al_2O_3 catalyst was supplied by Shell A/S, Fredericia, Denmark. Dichloromethane (DCM) (99.9% purity) and acetone solvents used in product separation were purchased from VWR. All the substances used to quantify the bio-crude and hydrotreated oil products (listed in Table S2†) were purchased from Sigma-Aldrich.

2.2. Experimental method

2.2.1. Hydrothermal liquefaction. All HTL experiments were carried out in a 400 mL stainless steel autoclave reactor in duplicates. The schematic view of the autoclave reactor is visualized in Fig. S1a.† Based on the optimized HTL condition in our previous studies, 234 g of homogeneous biopulp slurry containing around 38 g of the dry matter (ash-free) was injected into the reactor (~20% of dry matter) in the reference run (C0).[20,22] The reactor was then fully purged using N_2 gas to minimize the oxidization and subsequently pressurized up to 2 MPa. A 1.75 kW electrical ceramic heater with a 4 K min^{-1} heating rate was employed to maintain the desired operational temperature (350 °C). The operating HTL conditions have been optimized in our above-mentioned previous studies. The reactor constituents were uniformly mixed throughout the experiments using an internal stirrer. After completing the reaction (15 min residence time), the heater was promptly removed, and a compressed air system was implemented to accelerate the cooling rate. Nevertheless, due to the lower heat transfer capacity of the utilized autoclave reactor, the cooling

rate was relatively slow (5 K min^{-1}) in comparison to its micro-batch counterparts employed in our previous study.[22] As further discussed in the following sections, the lengthy heating/cooling rates expose the products to the hot medium, which might render unexpected variations in the structure of the HTL products.

The aqueous phase was thoroughly discharged through a syringe, while the solid and bio-crude phases were rinsed using 100 mL of DCM.[23] The obtained mixture was then filtered to separate the solid fragments following a decantation unit that facilitated the removal of water traces. The separation procedure is extensively elaborated elsewhere.[22] The extra water of the recovered aqueous phase was partially evaporated employing a lab-scale vacuum rotary evaporator (Büchi R210), where the temperature was isothermally kept at 65 °C while pressure was gradually decreased to 60 mbar. To tackle the foaming risk during operation, ten droplets of *n*-octanol were added to the round bottle flask to suppress foaming during the process.[24] The evaporation ceased once the water content was maintained according to the slurry. For the consecutive cycles (C1 to C3), the concentrated aqueous phase from the previous cycle along with biopulp was loaded to the reactor, building up the initial input slurry weight with the same water content.

2.2.2. Hydrotreating. Hydrotreating experiments were conducted in two 25 mL stainless steel micro-batch reactors (Swagelok) to ensure the comparability and reproducibility of the results. A simplified model of the autoclave reactor setup is shown in Fig. S1b.† The measured quantity and corresponding error of hydrotreated products were illustrated by the mean value and standard deviation, respectively, as a standard statistical representation method. Each rector was charged with around 4 g of produced bio-crude (from cycles C0 and C3) and 2 g of pre-activated Ni–Mo/Al_2O_3 catalyst. Four stainless steel spheres were added to the reactor to ensure the uniform mixing of the bio-crude during the reaction. The reactors were then pressurized with H_2 at (80 ± 3 bar). The utilized hydrotreating conditions are in accordance with the results of previous studies.[14,15,25]

The fully sealed reactors were then submerged into an SBL-2D fluidized sand bath (Techne, Stone, UK) equipped with a mechanical agitator (450 min^{-1}) for the desired residence time (3 h). The reactors were quenched into an ambient temperature water bath for 30 minutes. Correspondingly, the gas phase was initially sampled and vented prior to extracting other products. The flowable constituents of the reactor and the catalyst were passed through a metallic mesh without the intervention of any solvent and collected in a vial. The vial containing the oil and aqueous phase was centrifuged (4000 rpm – 5 min) to separate the hydrotreated oil (used for the analyses) and water content. The remaining products were thoroughly rinsed through acetone and filtered using a 5–13 μm filter paper. The residual catalyst and formed coke were collected and dried in the oven at 105 °C overnight. The quantity of the formed coke was determined by the difference between the obtained solids after the reaction and the input catalyst. Finally, the oil–solvent mixture was placed in a vacuum evaporator (Büchi R210) at 65 °C and 500 mbar. The total recovered oil was assumed to be the summation of the direct and acetone-washed oil phases. Fig. 1 represents the flowsheet of the APR-assisted HTL and HT processes.

2.3. Characterization and analysis techniques

Thermogravimetric analysis was performed employing a DSC/TGA system (Discovery SDT 650) to disclose the boiling point distribution of the bio-crudes compounds. The instrument was programmed as (1) 25 to 775 °C at 10 K min^{-1} heating rate, (2) isothermally heating at 775 °C for 30 min under an inert atmosphere (N_2), and (3) switching the inert gas to O_2 while maintaining the isothermal conditions at 775 °C.[26] Following the ASTM-D5291 standard procedure, the elemental composition of bio-crude, hydrotreated oil, and solid residue samples was monitored using an elemental analyzer (PerkinElmer, 2400 Series II, CHNS/O). Carbon, nitrogen, and hydrogen were directly determined, while oxygen content was determined by difference, assuming negligible sulphur content.[27] The higher heating value (HHV) of the hydrotreated oil and bio-crude samples was calculated *via* the Channiwala and Parikh correlation.[28] The boiling point distribution of the hydrotreated oil, as well as C0 and C3 bio-crude samples, was estimated through a simulated-distillation (SimDis) instrument complying with the ASTM-D7169. The instrument is equipped with a gas chromatography-flame ionization detector (GC-FID) (Shimadzu, Kyoto, Japan) and a Zebron ZB-1XT column (Phenomenex). The chemical composition of oil and aqueous samples was explored through the NIST database and a Varian gas chromatography (Thermo Scientific, Trace 1300)-mass spectrometry (ISQ-ID) (GC-MS) equipped with the CP-9036 and CP-3800 capillary columns, respectively. Quantification of specific amides and N-heterocyclic compounds in raw and hydrotreated bio-crudes was performed by gas chromatography (GC, Agilent 8890) coupled to a mass spectrometric (MS, Agilent 5977B) on a DB-5MS column (30 m × 0.25 mm × 0.25 mm). 1–10 mg of sample was therefore prepared in 1 mL of tetrahydrofuran (THF). An aliquot of 1 μL was injected at 300 °C in 1 : 20 split mode, using helium as carrier gas (1 mL min^{-1}). The column oven program started at 70 °C, which was held for 2 min, and progressed at 8 K min^{-1} until 180 °C and 4 K min^{-1} until 300 °C followed by a hold time of 2 min. Mass spectra were acquired in the SIM (selected ion monitoring) mode. Quantifier and qualifier ions are listed in Table S1.† Each analysis was repeated in triplicate, and the final values were averaged. The functionalities of the C0, C3 bio-crudes and all the hydrotreated oil samples were determined using a Fourier-transform infrared (FT-IR) (Bruker TENSOR II spectrometer) instrument in the range of 4000 to 400 cm^{-1}. Moreover, a Bruker Avance III 600 spectrometer operating at 150.9 MHz was employed to investigate the proton decoupled ^{13}C-NMR spectra of bio-crude and hydrotreated samples. In a typical run, around 25 mg of an oil sample was entirely dissolved in 100 mg of chloroform-d_1 ($CDCl_3$), poured into a specific quartz NMR vial, and introduced to the instrument. The baseline and phase corrections, peak integrations, and quantitative monitoring of the obtained spectrums were performed through MestReNova software.

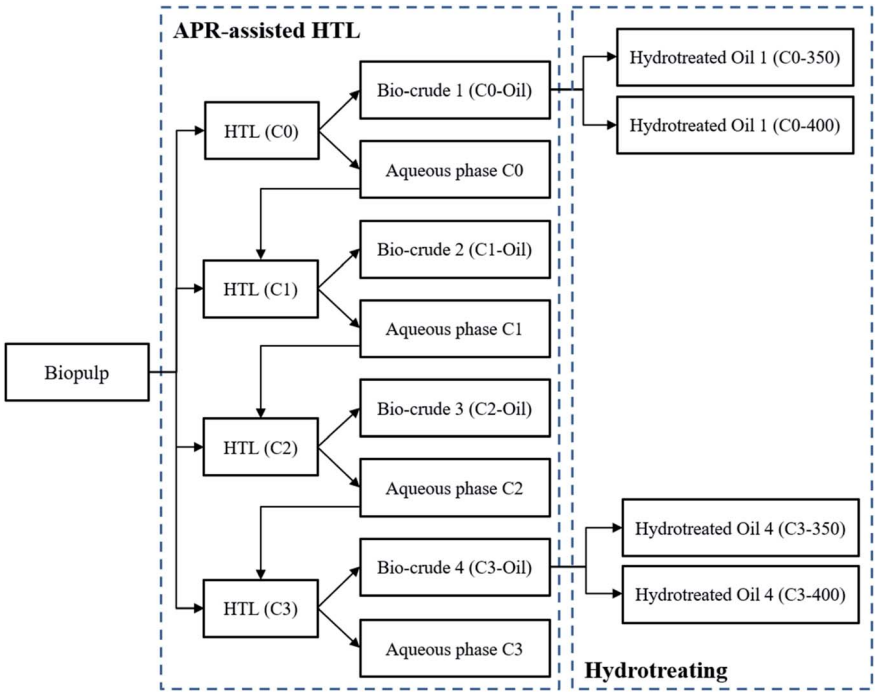

Fig. 1 Schematic view of the integrated HTL/HT processes.

Employing a Karl-Fischer instrument (Titroline 7500 KF), the water content of the concentrated aqueous phase samples was identified. The total organic carbon (TOC), total nitrogen (TN), and total ammonia (NH_4^+–N) were estimated through LCK386, LCK138, and LCK304 Hach kits, respectively aligned with a spectrophotometer instrument (Hach and Lange, DE3900). The gas composition of the HTL and HT experiments was characterized by a GC-2010 (Shimadzu Inc.) gas chromatograph equipped with a barrier ionization discharge detector (GC-BID) and a Supelco 1006 PLOT column using short (10 min) and long (25 min) duration methods, respectively.

The equation to calculate the product yield, energy recovery (ER), carbon and nitrogen recovery in the aqueous phase samples were defined elsewhere.[20] Note that the product distribution is calculated based on the biomass (DAF) as the denominator; therefore, the overall mass balance exceeds 100% depending on input concentrate. The deoxygenation (de-O) and denitrogenation (de-N) degrees were calculated based on eqn (1) and (2).

$$\text{De-O}(\%) = \left(1 - \frac{\text{O}_{\text{upgraded oil}}}{\text{O}_{\text{bio-crude}}}\right) \times 100 \quad (1)$$

$$\text{De-N}(\%) = \left(1 - \frac{\text{N}_{\text{upgraded oil}}}{\text{N}_{\text{bio-crude}}}\right) \times 100 \quad (2)$$

The H_2 consumption during the HT experiments was calculated following the ideal gas law based on the H_2 partial pressure measured before and after each experiment at room temperature (eqn (3)). The final H_2 partial pressure was determined based on the gas composition from GC-BID results. Volume V represents the part of the reactor which not occupied by the liquid.

$$n_{\text{consumed hydrogen}} = \frac{P_{\text{initial}} \times V}{\text{RT}} - \frac{P_{\text{final}} \times V}{\text{RT}} \quad (3)$$

The semi-quantitative GC-MS change index is calculated through eqn (4), where x and y represent the targeted bio-crude/hydrotreated bio-crude and Z indicates a specific compound in the oil samples.

$$\text{Change index}(x/y) = \frac{\text{Z}_x - \text{Z}_y}{\text{Z}_y} \times 100 \quad (4)$$

3. Results and discussion

3.1. Hydrothermal liquefaction

As shown in Fig. 1, three consecutive APR experiments followed the reference test to reveal the effect of aqueous phase recovery on product distribution. The bio-crude yield was conspicuously increased after the first cycle (7.3 wt%), whereas the solid residue yield remained consistent, relatively. Albeit the increasing trend in bio-crude yield was stabilized after C2, the bio-crude yield increased up to 41.8 wt% at the last cycle. The increasing trend in bio-crude yield after recirculation results from secondary HTL reactions such as condensation reaction.[3] In one hand, the hydrophilic amines originated from the decarboxylation of amino acids react with organic acids originating from the hydrolysis of lipids and carbohydrates to produce lipophilic amides.[29] On the other hand, the furfural derivatives resulting from the hydrolysis of carbohydrates react with ammonia to form heterocyclic nitrogen compounds.[30,31] The presence of amino acids originated from the high protein content of the biomass in the subsequent cycles, and their

reaction with the hydrolyzed building blocks of carbohydrates can also govern the formation of nitrogen heterocyclic species through the Maillard reaction. The reaction mechanism will be further explored in the following sections (Fig. 2).

The gas composition and produced pressure in all HTL experiments are shown in ESI (Fig. S2).† As asserted by Isa *et al.*, the produced light hydrocarbons can potentially vary the gas composition, while in this case, the inability of the employed method in detecting light hydrocarbons made the authors ignore the possible effect.[35] In contrast to the other phases, no clear trend was found for the gas phase. The gas sample from every cycle was dominated by CO_2 followed by H_2 and CH_4. The CO_2 proportion was slightly decreased during APR, possibly due to accelerated condensation reaction and lower availability of long-chain carboxylic acids in the subsequent cycles.

3.1.1. Analysis of HTL aqueous phase. The chemical composition of the fresh aqueous phases obtained by GC-MS is illustrated in Table 1. Acetic, levulinic, butanoic, and isovaleric acids were the most dominant light carboxylic acids in the aqueous phase samples. Moreover, 3-methyloxirane-2-carboxylic acid was only detected in the two subsequent cycles. The light organic acids are likely generated through the decomposition of carbohydrates during the HTL process. Upon recirculation, the relative peak area of the acids explicitly increased with the maximum quantity in the C3 aqueous phase, which explains the pH drop indicated in Fig. 3. The recovery of the acids to further cycles can facilitate the degradation of biomass macromolecules and form secondary reaction intermediates. As described by Abdelmoez *et al.* acidic HTL medium induces protein degradation and possibly form higher reactive condensation reaction precursors (*e.g.* amines).[32] The presence of glycerin reveals the occurrence of crude lipid hydrolysis that forms lipophilic straight-chain fatty acids. Various N-heterocyclic compounds have been detected in the aqueous phase samples. These N-heterocyclics likely result from the condensation and reduction of the Strecker degradation and Amadori rearrangement intermediate products. Another reaction proposed by Madsen *et al.* is the self-condensation of amino acids derived from the hydrolysis of protein macromolecules.[33] Pyrrolidinone derivatives are another abundant N-heterocyclic group. The formation of these compounds likely took place *via* the reaction of levulinic acid and ammonia.[34] Upon APR, the relative peak area of N-heterocyclic compounds, including pyrazine and pyrrolidinone derivatives, is significantly increased. This can be interpreted as the effect of higher acidic conditions during APR that accelerate the decomposition of protein precursors.[32] Alcohols were another abundant constituents of the aqueous phase stream that were likely formed through hydrolysis of lignin macromolecules. The produced alcohols might act as hydrogen donor compounds to form hydrogenolysis agent that ultimately lead to biomass depolymerization.[35] It should be noted that the employed GC-MS method does not provide a comprehensive overview of the aqueous phase samples and lacks the analysis of heavier compounds. Therefore, other analysis techniques such as pyro-GC, FT-ICR-MS, *etc.*, are required to explore the whole matrix of the aqueous samples.

To preclude the variation in the dry matter while recycling, the surplus water content of the obtained aqueous phases was removed through evaporation and then transferred to the next HTL run. Fig. 3a visualizes the significant increasing trends of TOC and TN, while NH_4^+–N exhibited a minor increase upon recycling. The TOC and TN of the aqueous phase obtained from C0 levelled to 17.44 and 3.23 kg m^{-3}, respectively. The values significantly increased to 27.5 and 4.9 kg m^{-3} in C1; however, after C2 an asymptotic behaviour was observed, likely due to saturation of water-soluble organics. As shown in our previous study, the saturation level of TOC occurred at around 61 kg m^{-3}, whereas herein, it happened at considerably lower levels (~27 kg m^{-3}).[20] The difference can be explained by the presence of alkali catalysts in that study, which promotes the production of light polar organics and elevates the TOC and TN saturation levels.[22] Furthermore, the pH values of each sample before and after surplus water removal were monitored. As it can be seen, the pH slightly decreased along with recirculation from 7.2 to 6.3. The addition of short-chain carboxylic acids originating from dehydration and decomposition of cellulose/hemicellulose to the next cycle can explain the pH reduction.[36]

Tracing the carbonaceous light organics loss during evaporation, the properties of all distillates and concentrates were also measured. Fig. 3b shows the TOC, TN, and NH_4^+–N distribution among the different phases (concentrate and distillate) obtained by aqueous phase evaporation. Around 77.8 to 83.2% of the organic carbon was associated with the concentrate phase, whereas noticeably fewer nitrogenous compounds (60.9 to 66.3%) fell under the same phase. Conspicuously, NH_4^+–N had a significant contribution in increasing the TN (22.4 to 30.0%) of the distillate phase. Along with consecutive APR, the NH_4^+–N revealed a tendency to remain in the concentrate phase, which points toward the pH dependency of NH_3/NH_4^+ equilibrium.[37] That is likely why C3 showed the highest TN fraction in its concentrate phase.

3.1.2. Analysis of HTL bio-crude. The elemental composition of biopulp, bio-crude, and solid residue samples are given in Table 2. The carbon and hydrogen content of the bio-crude samples were noticeably higher than those of the biomass.

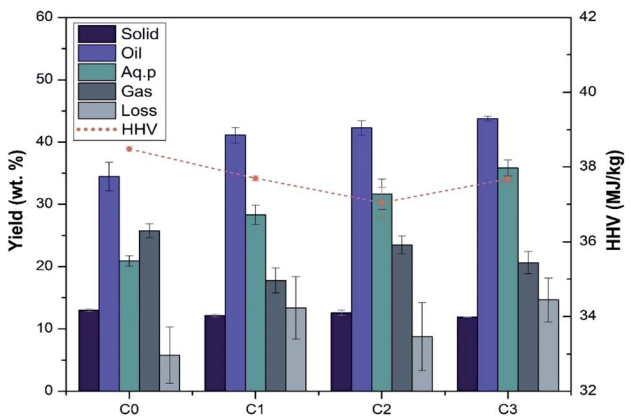

Fig. 2 Mass distribution and HHV of the bio-crude samples during sequential APR experiments.

Table 1 The chemical composition of the analyzed aqueous phase samples through GC-MS

Compound	Type	C0	C1	C2	C3
		Relative peak area (%)			
2-Heptanol, 3-methyl-	Alcohol	1.34	1.12	2.01	3.12
2,3-Butanediol	Alcohol	3.71	2.02	1.54	—
3-Methyl-5-methoxy-1-pentanol	Alcohol	—	—	—	2.01
1,3-Propanediol	Alcohol	1.85	2.44	2.61	3.6
5-Isopropenyl-2-methyl-7-oxabicyclo[4.1.0]heptan-2-ol	Alcohol	2.13	—	—	—
Glycerin	Alcohol	4.15	3.39	3.3	3.15
Dianhydromannitol	Alcohol	4.07	3.14	2.22	3.75
Isosorbide	Alcohol	2.38	2.1	1.82	—
Acetamide, *N*-ethyl-	Amide	1.43	1.38	1.57	1.94
2-Formylhistamine	Amine	1.26	1.35	1.34	1.17
4,4-Ethylenedioxy-1-pentylamine	Amine	1.94	—	—	—
Acetic acid	Carboxylic acid	7.85	7.15	9.65	10.87
3-Methyloxirane-2-carboxylic acid	Carboxylic acid	—	—	0.86	1.35
Levulinic acid	Carboxylic acid	0.98	1.45	1.24	1.89
Isovaleric acid	Carboxylic acid	0.97	1.54	1.43	2.01
Butanoic acid	Carboxylic acid	2.13	2.02	2.78	3.14
2-Cyclopenten-1-one, 2-methyl-	Ketone	2.25	2.03	2.45	2.58
2-Cyclopenten-1-one, 2,3-dimethyl-	Ketone	—	1.54	—	1.99
Spiro[2.4]heptan-4-one	Ketone	2.38	—	2.12	3.22
1*H*-Pyrrole, 2,5-dihydro-1-nitroso-	N-Heterocyclic	—	—	—	2.07
1,4-Dihydro-4-imino-1-methylaminopyridine	N-Heterocyclic	1.28	—	—	—
Pyrazine	N-Heterocyclic	0.98	1.65	1.87	2.13
3,7-Diazabicyclo[3.3.1]nonane, 9,9-dimethyl-	N-Heterocyclic	—	—	—	1.54
Pyrazine, methyl-	N-Heterocyclic	0.81	0.95	1.56	1.23
Piperidine, 2,3-dimethyl-	N-Heterocyclic	3.97	—	—	1.48
2-Pyrrolidinone, 1-methyl-	N-Heterocyclic	4.54	4.34	3.95	4.95
1-Ethyl-2-pyrrolidinone	N-Heterocyclic	4.66	5.12	5.18	6.25
2-Pyrrolidinone	N-Heterocyclic	3.17	4.15	4.9	5.1
3-Pyridinol, 2,6-dimethyl-	N-Heterocyclic	4.66	3.29	3.15	3.01
Pyrrolidine, 1-acetyl-	N-Heterocyclic	—	1.75	—	2.46
2-Piperidinone	N-Heterocyclic	2.19	2.15	3.09	3.34
Cyclohexanepropanenitrile, 2-oxo-	Nitrile	1.58	—	—	—

This is likely due to the hydrolysis of the biomass macromolecules to intermediates constituents (*i.e.*, monosaccharides, oligomers, fatty and amino acids) – and subsequently, the dehydration, deamination, decarboxylation, and decomposition of these intermediates to the bio-crude range compounds.[38] Hence, the bio-crude samples possessed less nitrogen and

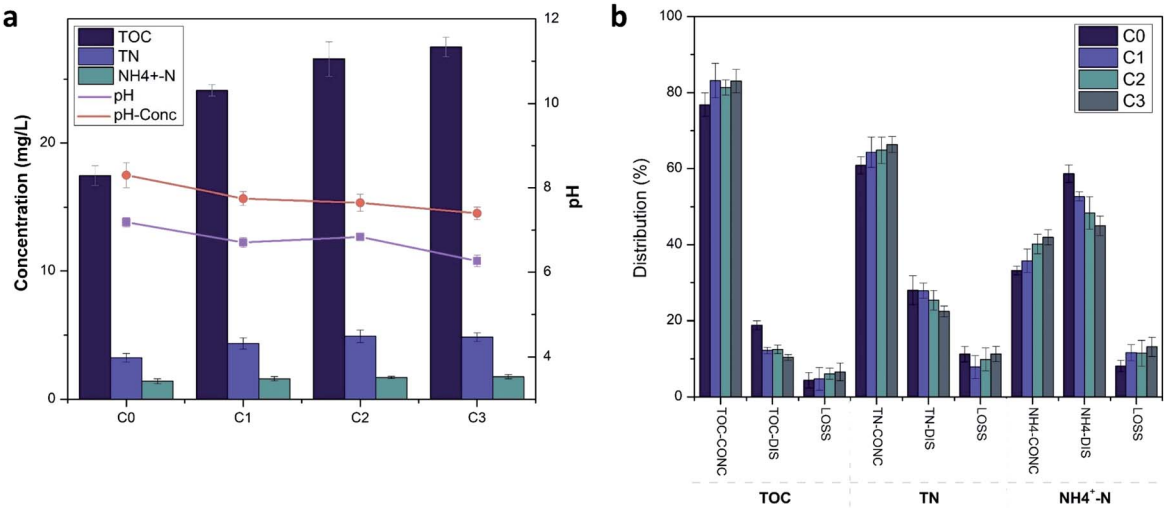

Fig. 3 (a) Properties of aqueous phases obtained from different cycles and (b) transformation of TOC, TN, and TH_4^+–N during aqueous phase concentration.

Table 2 Elemental analysis, ash content, higher heating value, and energy recovery of biopulp, bio-crude, and solid residue samples

Exp. (unit)	C (wt%)	H (wt%)	N (wt%)	O (wt%)	H/C (—)	N/C (—)	O/C (—)	Ash (wt%)	HHV (MJ kg^{-1})	ER (%)
Biopulp	51.70 ± 0.40	7.50 ± 0.10	3.30 ± 0.10	27.80 ± 0.60	1.74	0.058	0.403	9.70 ± 0.45	23.20 ± 0.02	—
C0-oil	76.61 ± 0.25	10.59 ± 0.01	4.08 ± 0.02	8.73 ± 0.28	1.66	0.049	0.085	0[a]	38.48 ± 0.06	57.16
C1-oil	75.13 ± 0.26	10.37 ± 0.06	5.07 ± 0.30	9.45 ± 0.63	1.66	0.062	0.094	0[a]	37.70 ± 0.07	66.81
C2-oil	74.15 ± 0.54	9.99 ± 0.30	5.27 ± 0.11	10.60 ± 0.94	1.61	0.065	0.10	0[a]	37.68 ± 0.41	67.54
C3-oil	74.79 ± 0.16	10.49 ± 0.07	5.39 ± 0.07	9.33 ± 0.30	1.68	0.066	0.093	0[a]	37.68 ± 0.01	71.10
C0-solid	29.96 ± 0.38	2.34 ± 0.06	1.59 ± 0.03	34.36 ± 0.41	0.94	0.050	0.86	31.75 ± 0.70	16.15 ± 0.11	9.14
C1-solid	29.15 ± 0.35	2.07 ± 0.01	1.34 ± 0.09	27.69 ± 0.33	0.85	0.042	0.71	39.76 ± 0.57	14.92 ± 0.14	7.89
C2-solid	31.87 ± 0.65	2.60 ± 0.09	1.33 ± 0.12	25.91 ± 0.61	0.98	0.038	0.61	38.29 ± 1.47	16.28 ± 0.37	8.92
C3-solid	29.46 ± 0.57	2.50 ± 0.08	1.1 ± 0.01	24.67 ± 1.85	1.02	0.034	0.63	42.28 ± 1.20	15.23 ± 0.09	7.90

[a] Assumed to be zero according to Fig. 4.

oxygen contents than biopulp. Upon APR, the carbon content of bio-crude marginally decreased, whereas no specific trend for hydrogen content was detected with a fluctuation between 10.0 to 10.6 wt% across various cycles. The reduction of carbon content is likely due to the built-up nitrogen and oxygen that were undesirably increased due to APR. In line with many previously published studies, recirculation of the aqueous phase caused higher nitrogen content in the C3 bio-crude.[3,39] Herein, C0 and C3 respectively showed 4.1 and 5.4 wt% of nitrogen content, possibly due to the formation of lipophilic amides and N-containing heterocyclic compounds in the subsequent cycles. Compared to our previous study and considering the identical operation conditions, the obtained bio-crude shows a higher nitrogen content (4.1 and 5.1 wt%, compared to 3.4 and 4.3 wt% in the two first cycles, respectively).

The reason likely corresponds to the types of employed reactors (autoclave *vs.* micro-batch) with different heating and cooling ramps. As mentioned before, the utilized autoclave reactor has a heating and cooling rate of 4 and 5 K min^{-1}, respectively, while the micro-batch reactor with a thinner wall diameter (3 mm) had drastically shorter temperature ramps. This condition can practically increase the exposure time of organic molecules in the low-temperature HTL reactor and drastically facilitate the repolymerization reaction leading to higher bio-crude yield and heteroatom content.[40] Luo *et al.* observed a similar trend while hydrothermally treating soy protein in short and long residence times.[41] Motavaf *et al.* asserted that in the prolonged batch holding times, the hydrophilic nitrogen-containing compounds such as amino acids dimerize together and/or react with monosaccharides to form nitrogen-rich molecules that contribute to the bio-crude phase.[42] As reported by Kristianto *et al.*, the formation of pyrazine derivatives reached a plateau at around 260 °C and slightly decreased at 280 °C.[43] Hence, the low heating rate of the autoclave reactor used in this study could accelerate the generation of the N-containing compounds. Therefore, due to transferring nitrogenous molecules from the aqueous phase to the bio-crude phase, along with nitrogen content, the bio-crude yield gets increased. The obtained results in this study explicitly support the hypothesis, where in comparison to the previous study, the bio-crude yield in C0 and C1 were increased by 12.4 and 16.9%, respectively.

As shown in Table 2, the bio-crudes obtained from the consecutive experiments revealed a higher O/C ratio, while H/C did not vary accordingly. Moreover, the N/C ratio was significantly enhanced upon recycling the concentrated process water due to elevated nitrogen content and the reverse carbon content trend. The N/C ratio in C0 was 0.05, whereas in C3, it levelled up to 0.07. Therefore, the HHV values for bio-crude samples were slightly reduced, resulting from the higher heteroatoms intake in the subsequent bio-crudes. However, due to the significant increment of bio-crude yield, the energy recovery was positively affected and ended up at 71.1% in the last cycle.

The results of carbon and nitrogen distribution are presented in Fig. S4.† Upon APR, the carbon yield in C3 bio-crude was 55.9 wt%, around 4.1 wt% higher than the reference experiment. However, in line with the results indicated in Fig. 3, higher carbon was concentrated in the aqueous phase recovered from the succeeding experiment. Nitrogen content followed the same trend as carbon. During APR, the nitrogen content of the bio-crude continuously increased and levelled up to 42.2 wt% in the last cycle, which was 5.3 wt% more than what is found in C0 bio-crude.

The boiling point distribution of bio-crude samples resulting from the thermo-decomposition and evaporation of various compounds is presented in Fig. 4a and b. The global thermogravimetric behaviour of bio-crude can be deduced by comparing the obtained results with the distribution curves reported in the literature.[44,45] In general, in all cases, more than 64.0% of the bio-crude was volatilized before 340 °C, potentially indicating a promising precursor for drop-in fuel production. Interestingly, minor volatilization was observed before 100 °C, revealing precise water and solvent (DCM) separation. The gasoline fraction (<193 °C) was slightly affected by APR. Hence, 11.5% of C3-oil was volatilized before 193 °C, which is higher than that of C0-oil (6.5%). The weight loss corresponding to jet fuel fraction (193–271 °C) in C3-oil was drastically increased compared to the bio-crudes obtained from the initial cycles. The variation in the gasoline and jet-fuel content of the bio-crude resulting from the succeeding cycles is likely due to the condensation of light heteroatomic compounds in bio-crude facilitated by APR. The results reported by Ramos-Tercero *et al.* are in line with the findings of this study.[46] C2 and C3 display a higher share of diesel fraction (272–425 °C) than those in C0 and C1. On the other hand, and as visualized in Fig. 4b, C0 and C1 showed

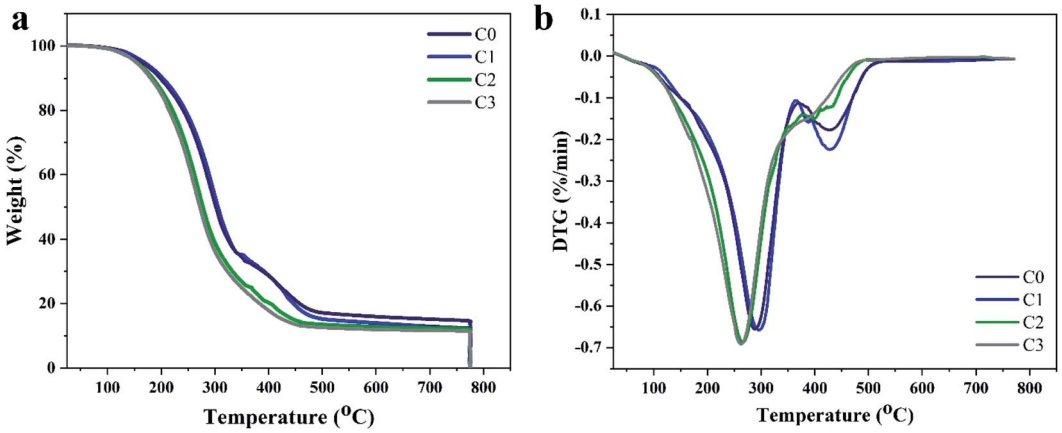

Fig. 4 (a) TG and (b) DTG curves of all bio-crude samples under N_2 (25–775 °C) and O_2 (≥775 °C).

a remarkable peak in the vacuum gas oil temperature (426–564 °C) range, whereas the C2 and C3 revealed relatively lower weight loss in this temperature range.

As mentioned before, the carrier gas was switched to O_2 at 775 °C, and residual fixed carbon was combusted for 30 min. Thereby, all the curves levelled down to zero, which shows the negligible ash content in all bio-crude samples.

3.2. Hydrotreating

The bio-crudes obtained in the reference experiment (C0) and the last cycle (C3) represent the impact of APR on the HTL process and therefore were selected for the hydrotreating experiment. The effect of hydrotreating temperatures (350 and 400 °C) and APR on the mass distribution in various hydrotreating output streams is discussed in Section 3.2.1. The heteroatom removal, H_2 consumption and overall carbon and nitrogen distributions throughout hydrotreating of the bio-crude samples are subsequently presented in Section 3.2.2. Lastly, the properties of hydrotreated bio-crudes are comprehensively elaborated in Section 3.2.3.

3.2.1. Effect of temperature and bio-crude feedstock on mass distribution. Fig. 5 visualizes the distribution of hydrotreating products, ranging from the hydrotreated oil to the water phase. Overall, more than 93% of the initial mass was recovered throughout different products, disclosing the high precision of separation and product collection methodologies. In general, the coke formation in this study is considerably high (6.7 to 11.7 wt%). Accelerated coke formation is reasonably favoured by the mass transfer limitations and thus nonuniform hydrogen dispersion resulting from the batch hydrotreating reactors.[47] Fig. 5 indicates that the temperature significantly affected the mass distribution of the hydrotreating products regardless of the bio-crude feedstock. Hydrotreating at 350 °C led to lower coke formation, while varying the temperature to 400 °C caused a consistent increase in coke formation. At C0-350 and C3-350, 6.7 and 7.1 wt% of coke were formed, while C0-400 and C3-400 yielded around 11.2 and 11.7 wt% of coke, respectively. This is in line with the study conducted by Haider *et al.*, where it was observed that when HTL bio-crudes are directly subjected to higher hydrotreating temperatures (400 °C), they may experience thermal instability, which results in higher coke formation.[17] Compared to C0, C3 bio-crude enhanced coke formation, likely resulting from the variation of bio-crude chemical composition caused by APR. The reactive oxygenated functional groups and aromatics make the bio-crude prone to cracking, polymerization, and condensation reactions that ultimately generate higher coke. As reported in Table 1, the aqueous phase recirculation increased the oxygen content and O/C of C3 bio-crude, while the aromaticity of the C3 did not change substantially (almost equivalent H/C), leading to a slight increase in coke formation upon APR.

As shown in Fig. 5a and b, regardless of the bio-crude feedstock, the severity of the reaction determined the gas yield and carbon loss in gaseous products. Light hydrocarbons, unreacted hydrogen, carbon monoxide, and carbon dioxide were the main gaseous constituents recovered after hydrotreating. C0-350 and C3-350 respectively corresponded to 6.6 and 8.6 wt% of gas, while operating at the higher temperature, increased the gas formation to 12.0 and 12.4 wt%, primarily due to the enhancement of the reverse water–gas shift and cracking reactions. Higher *n*-butane, propylene, ethane, and methane production caused higher carbon loss in the gaseous phase (Fig. 5b). Upon APR, the gas formation is increased in both 350 °C and 400 °C conditions. As an instance, the total gas formation enhanced from 6.6 wt% in C0-350 to 8.6 wt% in C3-350. The carbon loss in CO/CO_2 revealed a minor variation, whereas a significant carbon loss (gaseous hydrocarbons) was monitored after hydrotreating the bio-crude achieved from consecutive APR (C3). The observation clearly shows the vulnerability of the organic constituents conjugated to the bio-crude molecules by aqueous phase recirculation towards cracking. By comparing C0-400 and C3-400, an analogous trend is evident.

As described by Melero *et al.*, HDO reaction is directly related to the hydrotreating severity and hydrogen consumption. As reported that higher temperature accelerates HDO reaction and subsequently supports oxygen removal and water production.[48]

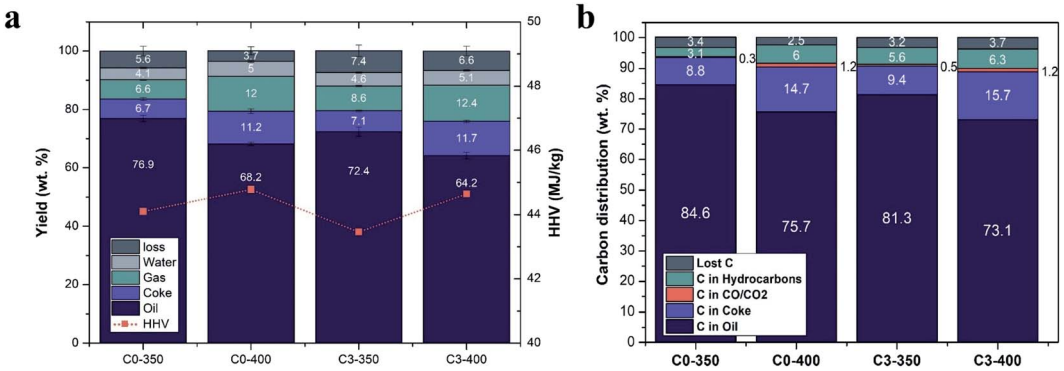

Fig. 5 (a) Products distribution and HHV and (b) carbon distribution among different hydrotreatment products.

In this study, water production is expectedly increased when operating under severe conditions. Hydrotreating at 350 °C formed 4.1 and 4.6 wt% of water, while operating at 400 °C, increased the values to 5 and 5.1 wt% in C0 and C3, respectively. Additionally, as a result of APR and consequently a greater extent of available oxygen in C3, a higher quantity of water was formed than that in C0.

3.2.2. Heteroatom removal, H_2 consumption, and C/N distributions. Heteroatom removal stands for the most challenging facet of bio-crude hydrotreating. Table 3 exhibits the elemental analysis results, heteroatom removal, and hydrogen consumption, along with the calculated calorific value of the hydrotreated bio-crudes. Albeit neither oxygen nor nitrogen was removed entirely in any hydrotreated bio-crude, a substantial heteroatom removal has occurred in all experiments. Despite the bio-crude feedstock, de-O has shown relatively higher efficiency than de-N in all cases due to the activation energy and type of the carbon–nitrogen bonds.[49] The least de-O was achieved at C0-350 and C3-350 cases (96.17 and 97.81%, respectively). The oxygen removal was slightly elevated when the operating temperature was switched to 400 °C. However, due to operational and mass transfer limitations in batch hydrotreating, high temperatures govern cracking and coking reactions, which results in reduced oil yield and higher coke formation.[15] Moreover, a higher reaction temperature favours decarboxylation/decarbonylation reactions, resulting in lower O/C in hydrotreated oil and higher CO and CO_2 production.

In comparison to oxygen, nitrogen removal was considerably lower, showing the resistance of some nitrogenous organics toward hydrotreating. As a function of temperature, de-N was promoted while hydrotreating at the elevated temperature by 17.8% and 21.8% for C0 and C3 bio-crudes, respectively. Despite the higher de-N of C3 bio-crudes at both temperatures (C3-350 and C3-400) than its C0 counterparts, a higher nitrogen content (see Table 3) was still detected in the C3 hydrotreated oils.

It can be appreciated that APR resulted in different types of nitrogen species. The added/formed nitrogen-containing compounds in the C3 bio-crude underwent hydrotreating and consumed more H_2 (higher de-N). On the other hand, some constituents remained in the hydrotreated oil phase and increased the nitrogen content. The type and quantity of different nitrogen species will be further discussed in Section 3.2.3. Fig. 6 illustrates the overall mass distribution of carbon and nitrogen while hydrotreating at 350 °C. As evidenced, APR increased the carbon content in bio-crude by 4.2 wt%. However, after hydrotreating, the higher amount of produced gases and higher heteroatom content mainly decreased the carbon content deference between C0 and C3 and reduced it to 1.7 wt%. Furthermore, recycling the concentrated process water led to a significant nitrogen association to the C3 bio-crude (5.1 wt% higher than C0), while hydrotreating managed to level it down to around 1.5 wt%.

Fig. 7 indicates the carbon and nitrogen distribution affected by APR and hydrotreating at 400 °C. Along with the increment of

Table 3 Elemental analysis, ash content, production yield, higher heating value, heteroatoms removal, hydrogen consumption, and energy recovery of hydrotreated oil samples[a]

Exp. (unit)	C (wt%)	H (wt%)	N (wt%)	O (wt%)	De-O (%)	De-N (%)	H/C (—)	N/C (—)	O/C (—)	H_2 consumption (kg H_2 per kg feed)	Ash[b] (wt%)	HHV (MJ kg^{-1})	ER* (%)
C0-350	84.30 ± 0.17	12.52 ± 0.24	2.74 ± 0.42	0.44 ± 0.07	96.17	48.30	1.78	0.030	0.003	0.015	0	44.10	88.14
C0-400	85.06 ± 0.02	12.84 ± 0.01	2.03 ± 0.16	0.07 ± 0.02	99.45	66.09	1.81	0.022	0.001	0.017	0	44.78	79.31
C3-350	84.03 ± 0.52	12.06 ± 0.22	3.63 ± 0.20	0.28 ± 0.03	97.81	51.20	1.72	0.0 9	0.003	0.018	0	43.46	83.52
C3-400	84.81 ± 0.59	12.80 ± 0.15	2.27 ± 0.37	0.12 ± 0.02	99.17	73.01	1.80	0.024	0.001	0.021	0	44.64	76.06

[a] Based on the input bio-crude. [b] Based on TGA results.

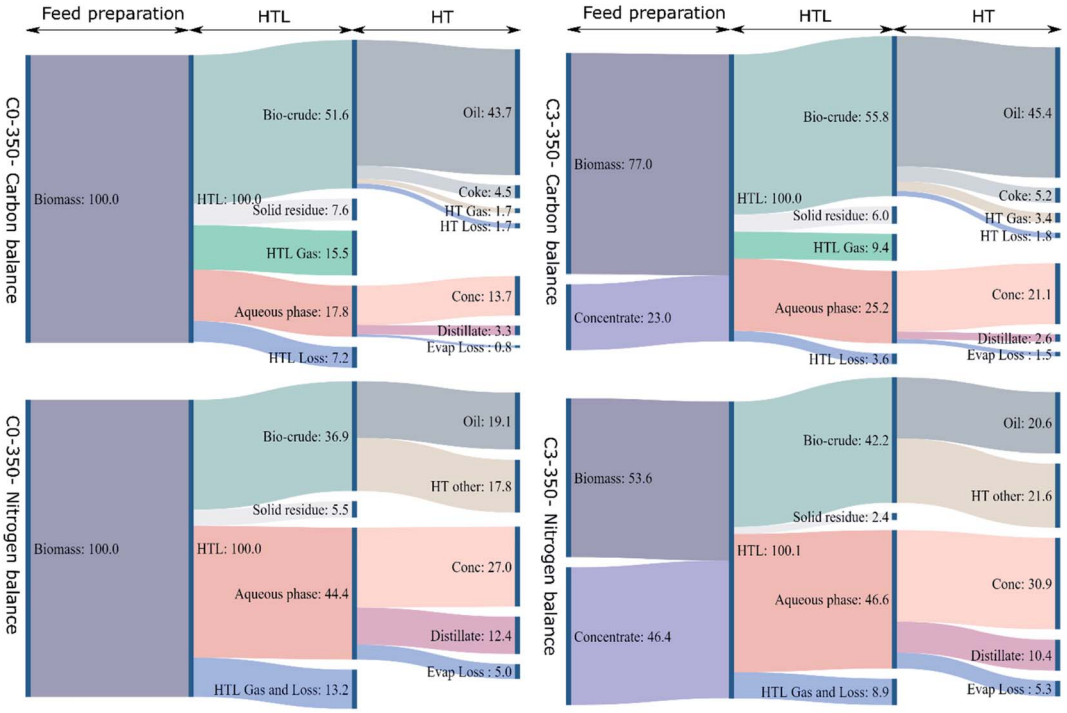

Fig. 6 Carbon and nitrogen distribution throughout the integrated HTL/HT process (calculated based on 100 g input of C or N).

hydrotreating severity (400 °C), the carbon distribution in C0-400 oil was significantly dropped in comparison to C0-350. This is mainly due to accelerated polymerization and condensation reactions that result in higher coke formation. Moreover, as described before, higher hydrotreating temperature promotes cracking reaction resulting in carbon loss in various light hydrocarbons. However, APR had a positive impact on carbon distribution in hydrotreated oil so that the carbon content in C3-400 hydrotreated oil was 1 wt% higher than its C0-400 counterpart. The elevated hydrotreating temperature revealed a greater de-N leading to lower nitrogen content in the final product. Taking C0 hydrotreated oil as an instance, C0-400 revealed 6.9 wt% less nitrogen than that in C0-350. The same trend was observed for C3 hydrotreated oil. In contrary to what was observed when hydrotreating at 350 °C, when applying APR, the C3-400 oil revealed lower nitrogen content (1 wt%) than C0-400 with the expense of higher H_2 consumption.

3.2.3. Analysis of the hydrotreated bio-crudes. Simulated distillation (SimDis) analysis was utilized to drive a comparison between the boiling point distribution of the C0 and C3 bio-crude samples with their corresponding hydrotreated oils. A better understanding of polymerization and cracking reactions in HTL and HT can be elucidated through the boiling point distribution curves obtained by SimDis. Fig. 8 visualizes the boiling point distribution of the samples, by which five different fractional cuts are determined (Table 4).

It can be concluded that upon APR, the C3 bio-crude is slightly more volatile than the C0 (higher recovery), particularly in the heavy diesel range. This is likely due to the higher condensation reactions of water-soluble compounds to form bio-crude-ranged molecules triggered by APR.[50] These results are in line with the information given in Fig. 4. Note that the deviation of SimDis and TGA results might be due to the cracking of the heavy compounds at higher temperatures and different calibration methods; therefore, these two methods cannot be directly compared. When the bio-crude is hydrotreated at 350 °C, the boiling point distribution noticeably shifts toward lighter fractions. Lower oxygen content in the hydrotreated oils than the bio-crude precursors due to major hydrodeoxygenation and moderate decarboxylation/decarbonylation potentially reduced the boiling point of the constituents of the hydrotreated oil.

Moreover, cracking can result in lower molecular weight and shift the curve to the left side. The cracking effect is reflected explicitly in the boiling range of heavy diesel. The C0 bio-crude contained 41.1 wt% of the heavy diesel-range compounds, while it reduced to 18.1 wt% in C0-350. On the other hand, light diesel and jet-fuel were significantly increased after mild hydrotreating. The observation is rather conspicuous in the case of C3-350, where APR enhances the condensation reactions to generate lipophilic molecules. Hence it could be concluded that hydrotreating cracked the formed heavy diesel ranged molecules to produce lighter constituents.

Hydrotreating at 400 °C induced shifting of the heavy fractions toward lighter hydrocarbons. In both C0 and C3, running the hydrotreating experiment at the elevated temperature increased the share of gasoline and jet-fuel considerably due to further degradation of heteroatom-containing molecules. The light diesel fraction was slightly increased, whereas the amount of heavy diesel was reduced, revealing an approximately

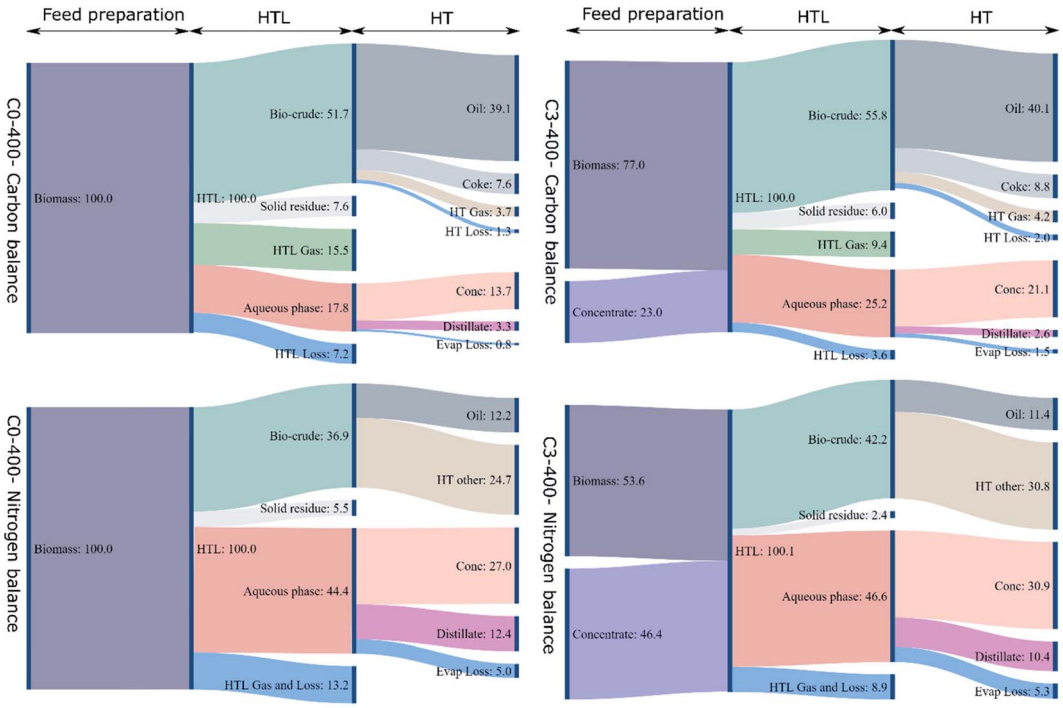

Fig. 7 Carbon and nitrogen distribution throughout the integrated HTL/HT process (calculated based on 100 g input of C or N).

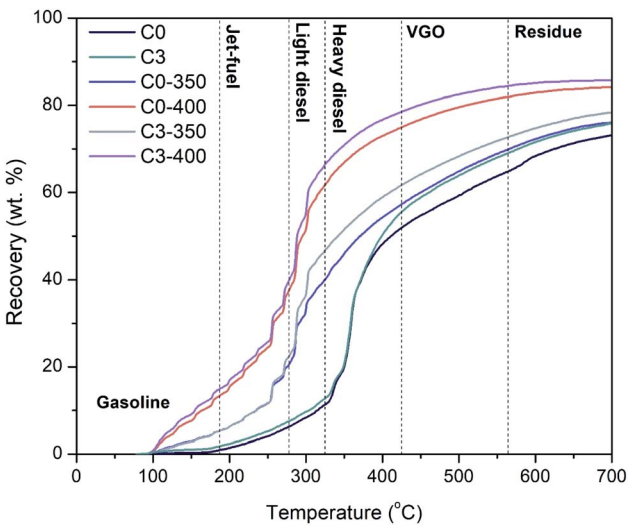

Fig. 8 Boiling point distribution of C0 and C3 bio-crude and the hydrotreated oil samples attained by SimDis (ASTM-D7169).

unchanged amount of diesel fractional cut with respect to that at 350 °C. Moreover, higher heteroatom removal efficiency associated with improved stabilization at 400 °C for both bio-crude samples significantly increased the overall recovery.

The chemical composition of bio-crude and hydrotreated oil samples was analyzed through GC-MS. Although the data obtained by GC-MS is limited by the volatility of the oil samples, it still points toward the composition of the fractions that fall under the potential drop-in fuels and/or bio-based blendstocks. Fig. 9 visualizes the qualitative results of the 60–70 most relevant volatile compounds (quantified by relative peak area) of the bio-crude and hydrotreated samples, categorized based on the organic functional groups. Furthermore, a full quantification of some representative class compounds is carried out to reveal the fate of different N-containing compounds.

Carboxylic acids were the most abundant components of the volatile fractions of bio-crude samples that accounted for more than 66% of the identified peak area, followed by amides, nitrogen heterocyclic compounds, and alcohols. The long-chain carboxylic acids were indeed the fatty acids that originated from the hydrolysis of the lipid content of the biomass. Hexadecanoic acid (C_{15}–COOH) and octadecanoic acid (C_{17}–COOH) were the predominant compounds in bio-crude samples originated from 1,2,3-tripalmitoyl glycerol and 1,2,3-tristearoyl glycerol, respectively. Although the qualitative analysis limits the relevance of peak area value to the absolute concentration, it still elucidates the influence of the reaction pathway throughout the HTL and/or HT processes.[8] Upon recirculation, the relative peak area of fatty acid compounds decreased in C3 bio-crude. On the other hand, a large proportion of the total peak area in C3 is represented by fatty acid amides. Hexadecanamide and *N*,*N*-dimethyl-octadecenamide verify the occurrence of condensation reaction during HTL. The condensation reaction consumes carboxylic acids and amines/ammonia (originated from the decarboxylation of amino acids and/or recirculated N-containing compounds) and forms fatty acid amides.[36] The second-largest majority of N-containing compounds was detected to be N-heterocyclic derivatives. Indole (2,3-dimethyl-indole, 3-methyl-indole), pyrazine (2-ethyl-5-methyl-pyrazine, 2,5-dimethyl-pyrazine), pyridine (2-ethyl-pyridine, 2,5-

Table 4 Fractional cuts attained by SimDis of C0 and C3 bio-crudes and hydrotreated oil samples

		Composition (wt%)					
Fractional cuts	Boiling point range	C0	C3	C0-350	C0-400	C3-350	C3-400
Gasoline	<193 °C	1.1	2	5.7	14	5.6	15.5
Jet-fuel	193–271 °C	4.7	4.9	12.8	19.5	13.3	20.2
Light diesel	272–321 °C	5.1	5.3	20.7	27.3	27	29.8
Heavy diesel	322–425 °C	41.1	43.3	18.1	14.2	15.8	13
VGO	426–564 °C	12.9	13.5	12.6	17	11	5.9
Residue	>564 °C	8.4	6.9	6.2	2.1	5.7	1.3
Overall recovery	75–700 °C	73.2	75.9	76.1	84.1	78.4	85.7

dimethyl-pyridine), and pyrrolidinone derivatives (1-ethyl-2-pyrrolidinone) were respectively the most abundant N-heterocyclics in bio-crudes. Despite the presence in both C0 and C3, the relative peak area of N-heterocyclic derivatives is seemingly given rise by aqueous phase recirculation, owing to the Maillard and condensation reactions.[31,39] The higher availability of free ammonium and other N-containing compounds in the subsequent HTL cycles likely explains the observed increment. The other abundant N-heterocyclic product was quinoline and its derivatives (2-methyl-quinoline, 2,6-dimethyl-quinoline), which were possibly formed by condensation of oxygenated aromatics (hydrolysis of lignin) and ammonia.[33]

As described by SimDis, hydrotreating at 350 °C did not considerably change the overall recovery, while the recovery of molecules in the potential drop-in fuel range increased remarkably. As can be seen in Table 4, higher recoveries of volatile compounds (below 350 °C) were observed in C0-350 (45.9 wt%) and C3-350 (51.5 wt%) than in C0 (20 wt%) and C3 (20.7 wt%). Moreover, a dramatic variation in the distribution of different functionalities is observed. By adopting hydrotreating at 350 °C, most fatty acids and fatty acid amides were converted to the corresponding hydrocarbons. The most noticeable change is related to the formation of the aliphatic compounds in the form of *n*-paraffins, followed by iso-paraffins. However, hexa- and octadecanamide were still presented in the C0-350 and C3-350 hydrotreated oil samples due to lower activation energy provided in mild hydrotreating experiments. Despite the predominance of hexa (C_{16}) and octadecane (C_{18}), pentadecane (C_{15}) and heptadecane (C_{17}) were also found in the bio-crudes hydrotreated at 350 °C. This phenomenon is in line with previous findings, where decarboxylation reaction took place in less severe hydrotreating conditions.[15,51] Occurrence of decarboxylation reaction results in the removal of one carbon atom and odd *n*-paraffinic chains in the hydrotreated oil. Biller *et al.* detected a significant share of hexadecanenitrile and octadecanenitrile while hydroprocessing of microalgae bio-crude at mild operating conditions resulted from dehydration of the amide precursors.[16] However, only traces of nitrile compounds (mainly octadecanenitrile) were found in this study. The N-heterocyclics were the most abundant nitrogenous compounds in C0-350 and C3-350 bio-crudes. The relative peak area of nitrogen-containing heterocyclics in C3-350 is slightly higher than in C0-350. The reaction mechanism for hydrodenitrogenation of aromatic N-heterocyclics involves

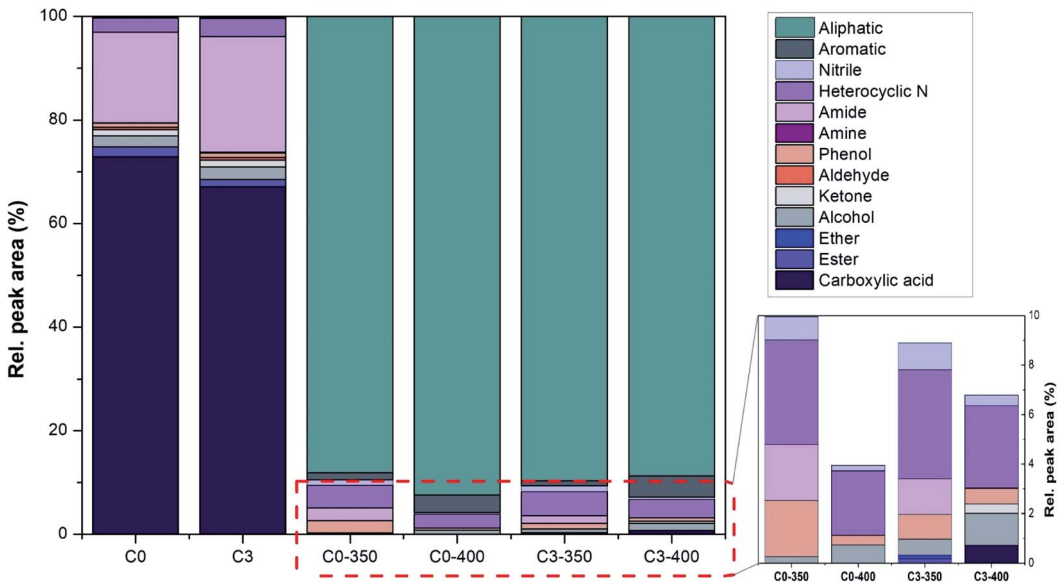

Fig. 9 The chemical composition of the analyzed oils through GC-MS in terms of different functionalities.

hydrogenation of the heteroring and subsequently C–N bond scission. The C–N bond in the heteroring with relatively close activation energy to that of C–N double bond makes C–N bond cleavage kinetically unfavourable.[52,53] Addressing the challenge of hydrotreating the aromatic nitrogenous molecules likely requires severe hydrotreating conditions and higher H_2 initial pressure.

Hydrotreating at 400 °C converted all the fatty acids and fatty acid amides to their conjugated straight-chain hydrocarbons, dominantly hexa (C_{16}) and octadecane (C_{18}). As introduced, severe hydrotreating condition tends to govern the heteroatom removal through hydrodeoxygenation. Moreover, the relative peak area of nitrile compounds was slightly diminished in C0 and C3. Despite applying severe hydrotreating conditions, the N-containing heterocyclics were still present in the hydrotreated bio-crude samples, contributing to the relatively lower de-N. Indole derivatives were the most abundant heteroaromatics that resisted hydrotreating.[54] In line with the elemental analysis results presented in Table 3, despite higher H_2 consumption and de-N, the peak area of N-containing compounds in the C3-400 hydrotreated oil was slightly higher than that of the C0-400, disclosing the adverse effects of APR on the chemical properties of the hydrotreated bio-crudes.

To illustrate the effect of APR on the fate of amides and N-heterocyclics in raw and hydrotreated bio-crudes, amides and N-heterocyclic compounds were quantitatively analyzed. Table S2† shows the absolute concentration of all subjected components. It should be noted that hydrotreating at 350 and 400 °C expectedly increases the concentration of lighter derivatives of N-heterocyclic compounds through cracking of complex alkylated poly-heterocyclics structures. Therefore, a higher concentration of the subjected N-heterocyclic compounds in a hydrotreated bio-crude does not imply that the nitrogen content is higher than in the bio-crude feed. Fig. 10 represents the impact of APR on the class representative N-compounds in bio-crudes and hydrotreated bio-crudes at different temperatures *versus* change index. As can be seen, the condensation of carboxylic acids and amines increased the amide concentration in C3 bio-crude (positive C3/C0 change index in representative amides). *N*-Ethyl octadecanamide (47.6%), *N*-methyl hexadecanamide (43.3%), *N*-ethyl hexadecanamide (34.0%), and octadecanamide (25.59%) showed the greatest increment among others. The concentration of N-heterocyclic compounds is also enhanced in all the representative class compounds. Indole (23.2%) and 2,6-dimethyl quinoline (21.8%) exhibited the most significant positive change, possibly due to the Maillard reaction between reduced sugars and amino acids and cyclization/dimerization of amino acids facilitated by APR.[55] A significant improvement in the concentration of amides was monitored in C3-350 than its C0 counterpart. The amount of *N*-methyl hexadecanamide is approximately increased by 360.2%. The same trend is observed for the N-heterocyclic compounds, where quinoline derivatives represented a significant positive change index. It clearly appreciates that hydrotreating at 350 °C does not associate with a remarkable hydrodenitrogenation, and thus harsher hydrotreating conditions are required. Hydrotreating at 400 °C, on the other hand, remarkably

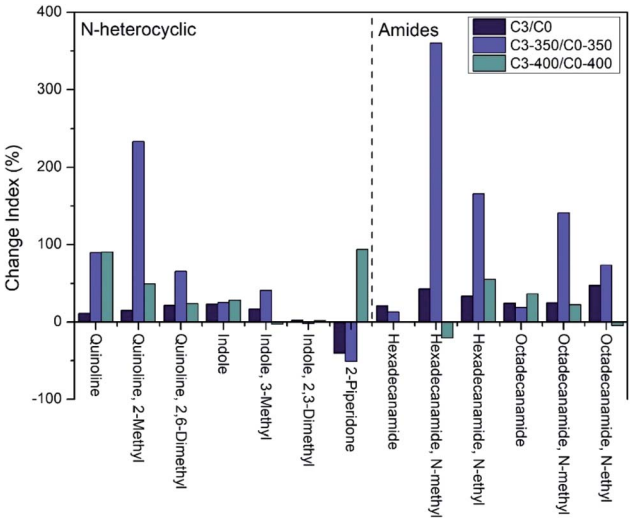

Fig. 10 Change index of nitrogenous class representative compounds.

diminished the positive change index of representative amides. *N*-Methyl hexadecanamide and *N*-ethyl octadecanamide are reduced by −20.7 and −4.6%, respectively, showing the efficiency of higher hydrotreating temperature on the removal of amides. On the other hand, the concentration of all the N-heterocyclic class representative compounds increased in C3-400 compared to C0-400. It conspicuously indicates the persistent nature of N-heterocyclic compounds toward hydrotreating even at elevated temperatures investigated in this study.

The results are in line with what was observed in Fig. 6 and 7, where hydrotreating at 350 °C resulted in higher overall nitrogen recovery in C3-350 oil than C0-350, whereas severe hydrotreating conditions slightly diminished the overall nitrogen distribution in the C3-400 hydrotreated oil than its C0 counterpart.

Fig. 11 presents the FT-IR spectra of the C0 and C3 bio-crude feedstocks and the hydrotreated oils at different temperatures. The broad and prominent peak within the range of 3500 to 3100 cm^{-1} is likely related to O–H stretching vibration, indicating the high oxidative functionalities in the bio-crude samples. Another detected strong peak at around 1710 cm^{-1} is attributed to the C=O stretching vibration of ketones, aldehydes, amides, and/or carboxylic acids. Comparing C0 and C3, although no significant variation is observed in the carbonyl vibration peak, a stronger peak was detected at around 3400 cm^{-1} in the case of C3. The N–H stretching peak at 3325 cm^{-1} signifies the occurrence of condensation reaction in the subsequent cycles utilizing long and short-chain carboxylic acids.

Hydrotreated bio-crudes, more specifically C0-350 and C3-350, revealed slight absorbances around 3300 and 1710 cm^{-1}, which corresponds to the incomplete heteroatom removal at mild operational conditions.[56] However, the broad peak from 1100 to 1300 cm^{-1}, revealing the presence of ester compounds in bio-crude, is removed in the hydrotreated bio-crude samples. In both cases, the higher reaction severity resulted in

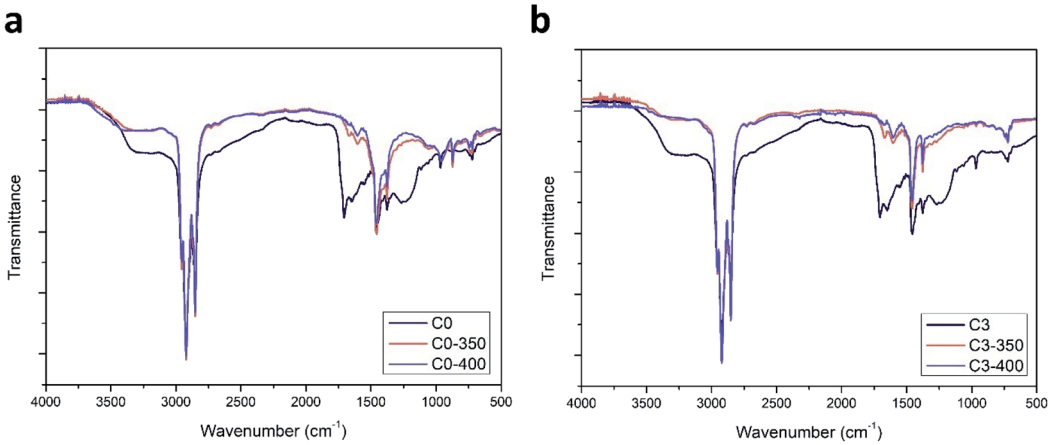

Fig. 11 FT-IR results of bio-crude and the corresponding hydrotreated oil samples of (a) C0 and (b) C3.

a negligible effect on the intensity of the oxygenates' peaks. This can support the de-O results, where the oxygen removal was above 96.2 wt% regardless of the operating temperature and feedstock. The sharp triple-band at 2940 cm^{-1}, 2920 cm^{-1}, and 2850 cm^{-1} is assigned to the C–H stretching vibration of the alkyl functional groups. The double bond peak at 1375 and 1450 cm^{-1} presents the C–H bending vibrations of alkane groups. The C=C stretching vibration peak appeared at around 1615 cm^{-1}, suggesting the presence of olefins and aromatics in the bio-crude samples, while the peaks are diminished in the case of hydrotreated oils. This clearly confirms the sufficient hydrogenation of the oils resulting in higher saturation and heating value (higher H/C).

^{13}C-NMR was utilized to clarify the conversion route of different cycles of bio-crude (C0 and C3) and characterize the corresponding hydrotreated oils based on the organic functionalities. The ^{13}C-NMR analysis provides valuable information on the type and relative carbon percentage conjugated to different functionalities (and heteroatoms) throughout the entire matrix of the analyzed oil samples. The qualitative evaluation of the presented functional groups in bio-crude and hydrotreated oil samples was carried out by integrating the specific regions of ^{13}C-NMR to various chemical shifts exhibited in Fig. S5.† Based on the particular chemical shift, the relative carbon content of each organic functional group is estimated and shown in Fig. 12. It should be noted that the carbon peak related to $CDCl_3$ at around 77.6 ppm is disregarded. The region 0–55 ppm corresponds to the aliphatic carbon atoms with the minimum two bond distance with the adjacent oxygen atom. However, the deshielding effect of nitrogen atoms might shift some nitrogen-bonded carbon atoms to this region.[57] The region is subdivided into 0–28 and 28–55 ppm representing the saturated short-straight chain and long-branched aliphatics, respectively. C0 and C3 bio-crudes showed relatively similar carbon atoms in the 0–28 ppm region, suggesting a negligible impact of APR on the carbon type of short aliphatics. However, C3 revealed relatively higher carbon atoms in the 28–55 ppm region, implying a higher branched aliphatics content. Hydrotreating, particularly at 400 °C, significantly increased the proportion of methyl carbons (shielding to upfield) by cracking the long-chain aliphatics. The peaks appeared at around 10 ppm suggest fewer branching points in C0-400 and C3-400 than the 350 °C counterparts. The region 55–95 ppm corresponds to the carbons adjacent to oxygen, mainly in the form of anhydrous carbohydrates, ethers, and alcohols. The relative carbon content in this region is slightly enhanced after APR, representing the higher oxygen build-up in the consecutive obtained bio-crude. Hydrotreating either at 350 or 400 °C led to removing the oxygen-containing functional groups that corresponded to negligible chemical shifts in 55–95 ppm. The integrated region 95–120 ppm mainly indicates the cyclic and acyclic olefins. All the analyzed oils revealed insubstantial chemical shifts in this region. The following chemical shift region lying between 120 and 150 ppm represents the aromatic and heteroaromatics hydrocarbons, including benzene derivatives. C3 bio-crude was attributed to a high chemical shift in this region (see Fig. 5a). The following downfield regions respectively correspond to substituted phenol, ester/carboxylic acid, and ketone/aldehyde derivatives. Lastly, hydrotreated oils exhibited insignificant chemical shifts in the

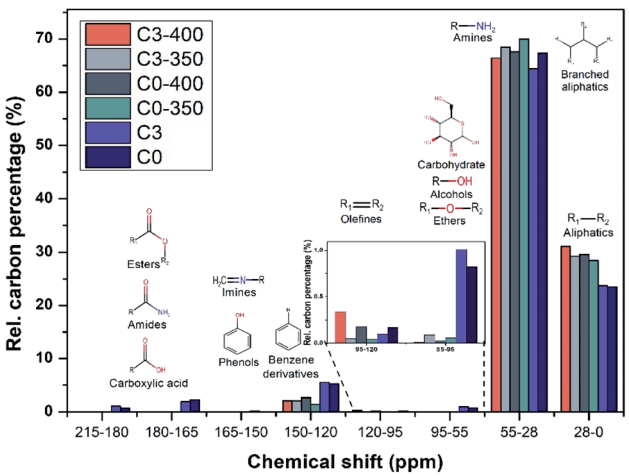

Fig. 12 Quantitative ^{13}C-NMR analysis results of bio-crudes (C0 and C3) and hydrotreated bio-crudes.

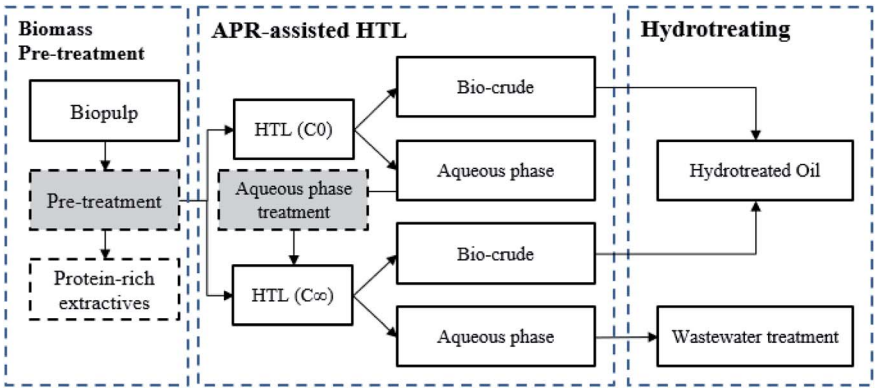

Fig. 13 The recommended strategy for the efficient valorization of protein-rich biomass through HTL.

two last downfield chemical shift regions confirming the occurrence of severe deoxygenation reactions under mild and harsh hydrotreating conditions.

4. Conclusion

By reducing up to 30% of nitrogenous compounds and less than 13% of organic carbon, aqueous phase concentration heralds a promising method that opens the possibility of aqueous phase recirculation (APR) while treating wet biomass. APR increased the bio-crude yield and energy recovery by 9.3 wt% and 13.9%, respectively. Furthermore, it also increased the carbon distribution in the subsequent cycle by 4.2 wt% compared to the reference bio-crude. On the other hand, APR resulted in higher nitrogen content (5.3 wt%), mainly in the form of fatty amides and heterocyclic N-containing compounds, which subsequently challenges the downstream processes. Hydrotreating the reference (C0) and subsequent (C3) bio-crudes at mild conditions (350 °C) resulted in higher carbon (1.7 wt%) and nitrogen (1.5 wt%) distribution in C3 hydrotreated oil. Therefore harsher hydrotreating condition was applied to the bio-crude precursors. Hydrotreating at 400 °C successfully reduced the number of fatty amides with the expense of higher H_2 consumption; however, the heterocyclic N-compounds remained a challenge. Furthermore, the carbon recovery in C3-400 (40.1%) remarkably decreased from that in C3-350 (45.4%), resulting in lower overall hydrotreated oil yield and energy recovery. Therefore, the adoption of severe hydrotreating conditions can make the process less economically feasible. The authors suggest that APR of protein-rich biomass requires one or a combination of the following strategies (as Fig. 13): (1) a biomass pretreatment process capable of extracting protein content needs to be integrated into the upstream value-chain. (2) An aqueous phase treatment process that eliminates the reactive N-containing compounds of the subjected aqueous phase before recirculation.

Author contributions

K. K.: conceptualization, data curation, formal analysis, investigation, methodology, roles/writing—original draft, visualization, writing—reviewing and editing; K. S.: investigation, formal analysis, methodology, writing—reviewing and editing; M. S. H.: conceptualization, methodology, writing—reviewing and editing; S. S. T.: methodology, writing—review and editing; D. C.: conceptualization, writing—reviewing and editing; J. Z.: formal analysis, writing—reviewing and editing; L. A. R.: conceptualization, funding acquisition, project administration; T. H. P.: conceptualization, funding acquisition, investigation, project administration, resources, supervision, validation, writing—reviewing and editing. All authors have read and agreed to the published version of the manuscript.

Conflicts of interest

The authors declare no conflict of interest.

Acknowledgements

This project has received funding from the European Union's Horizon 2020 Research and Innovation Programme under grant agreement no. 818413 (NextGenRoadFuels).

References

1 K. Kohansal, A. Tavasoli and A. Bozorg, Using a hybrid-like supported catalyst to improve green fuel production through hydrothermal liquefaction of Scenedesmus obliquus microalgae, *Bioresour. Technol.*, 2019, **277**, 136–147, https://www.sciencedirect.com/science/article/pii/S0960852418317528.

2 W. T. Chen, Y. Zhang, T. H. Lee, Z. Wu, B. Si, C. F. F. Lee, *et al.*, Renewable diesel blendstocks produced by hydrothermal liquefaction of wet biowaste, *Nat. Sustain.*, 2018, **1**(11), 702–710, DOI: 10.1038/s41893-018-0172-3.

3 S. Leng, L. Leng, L. Chen, J. Chen, J. Chen and W. Zhou, The effect of aqueous phase recirculation on hydrothermal liquefaction/carbonization of biomass: a review, *Bioresour. Technol.*, 2020, **318**, 124081, https://www.sciencedirect.com/science/article/pii/S0960852420313535.

4 P. Ranganathan and S. Savithri, Techno-economic analysis of microalgae-based liquid fuels production from

wastewater via hydrothermal liquefaction and hydroprocessing, *Bioresour. Technol.*, 2019, **284**, 256–265, https://www.sciencedirect.com/science/article/pii/S0960852419304468.

5 N. Hajinajaf, A. Mehrabadi and O. Tavakoli, Practical strategies to improve harvestable biomass energy yield in microalgal culture: a review, *Biomass Bioenergy*, 2021, **145**, 105941, https://www.sciencedirect.com/science/article/pii/S0961953420304736.

6 R. Cherad, J. A. Onwudili, P. Biller, P. T. Williams and A. B. Ross, Hydrogen production from the catalytic supercritical water gasification of process water generated from hydrothermal liquefaction of microalgae, *Fuel*, 2016, **166**, 24–28, https://www.sciencedirect.com/science/article/pii/S0016236115010984.

7 B. Si, L. Yang, X. Zhou, J. Watson, G. Tommaso, W.-T. Chen, *et al.*, Anaerobic conversion of the hydrothermal liquefaction aqueous phase: fate of organics and intensification with granule activated carbon/ozone pretreatment, *Green Chem.*, 2019, **21**(6), 1305–1318, DOI: 10.1039/C8GC02907E.

8 Z. Zhu, L. Rosendahl, S. S. Toor, D. Yu and G. Chen, Hydrothermal liquefaction of barley straw to bio-crude oil: effects of reaction temperature and aqueous phase recirculation, *Appl. Energy*, 2015, **137**, 183–192, DOI: 10.1016/j.apenergy.2014.10.005.

9 S. Leng, W. Li, C. Han, L. Chen, J. Chen, L. Fan, *et al.*, Aqueous phase recirculation during hydrothermal carbonization of microalgae and soybean straw: a comparison study, *Bioresour. Technol.*, 2020, **298**, 122502, https://www.sciencedirect.com/science/article/pii/S0960852419317328.

10 J. Chen, J. Zhang, W. Pan, G. An, Y. Deng, Y. Li, *et al.*, A novel strategy to simultaneously enhance bio-oil yield and nutrient recovery in sequential hydrothermal liquefaction of high protein microalgae, *Energy Convers. Manage.*, 2022, **255**, 115330, https://www.sciencedirect.com/science/article/pii/S0196890422001261.

11 A. A. Shah, S. S. Toor, T. H. Seehar, R. S. Nielsen, A. H. Nielsen, T. H. Pedersen, *et al.*, Bio-crude production through aqueous phase recycling of hydrothermal liquefaction of sewage sludge, *Energies*, 2020, **13**(2), DOI: 10.3390/en13020493.

12 H. Chen, Z. He, B. Zhang, H. Feng, S. Kandasamy and B. Wang, Effects of the aqueous phase recycling on bio-oil yield in hydrothermal liquefaction of Spirulina platensis, α-cellulose, and lignin, *Energy*, 2019, **179**, 1103–1113, https://www.sciencedirect.com/science/article/pii/S0360544219308230.

13 G. W. Huber and A. Corma, Synergies between Bio- and Oil Refineries for the Production of Fuels from Biomass, *Angew. Chem., Int. Ed.*, 2007, **46**(38), 7184–7201, DOI: 10.1002/anie.200604504.

14 M. S. Haider, D. Castello, K. M. Michalski, T. H. Pedersen and L. A. Rosendahl, Catalytic hydrotreatment of microalgae biocrude from continuous hydrothermal liquefaction: Heteroatom removal and their distribution in distillation cuts, *Energies*, 2018, **11**(12), DOI: 10.3390/en11123360.

15 D. Castello, M. S. Haider and L. A. Rosendahl, Catalytic upgrading of hydrothermal liquefaction biocrudes: Different challenges for different feedstocks, *Renewable Energy*, 2019, **141**, 420–430, DOI: 10.1016/j.renene.2019.04.003.

16 P. Biller, B. K. Sharma, B. Kunwar and A. B. Ross, Hydroprocessing of bio-crude from continuous hydrothermal liquefaction of microalgae, *Fuel*, 2015, **159**, 197–205, DOI: 10.1016/j.fuel.2015.06.077.

17 M. S. Haider, D. Castello and L. A. Rosendahl, Two-stage catalytic hydrotreatment of highly nitrogenous biocrude from continuous hydrothermal liquefaction: a rational design of the stabilization stage, *Biomass Bioenergy*, 2020, **139**, 105658, https://www.sciencedirect.com/science/article/pii/S0961953420301926.

18 M. D. Argyle and C. H. Bartholomew, Heterogeneous catalyst deactivation and regeneration: a review, *Catalysts*, 2015, **5**(1), 145–269.

19 C. Kwak, J. J. Lee, J. S. Bae and S. H. Moon, Poisoning effect of nitrogen compounds on the performance of CoMoS/Al2O3 catalyst in the hydrodesulfurization of dibenzothiophene, 4-methyldibenzothiophene, and 4,6-dimethyldibenzothiophene, *Appl. Catal., B*, 2001, **35**(1), 59–68, https://www.sciencedirect.com/science/article/pii/S0926337301002338.

20 K. Kohansal, S. Toor, K. Sharma, R. Chand, L. Rosendahl and T. H. Pedersen, Hydrothermal liquefaction of pre-treated municipal solid waste (biopulp) with recirculation of concentrated aqueous phase, *Biomass Bioenergy*, 2021, **148**, 106032, https://www.sciencedirect.com/science/article/pii/S0961953421000696.

21 P. Fritzel, *ECOGI Pre-treatment of biomass for anaerobic digestion*, 2015, vol. 1005, pp. 1–37, http://ecogi.dk/wp-content/uploads/2019/12/Testrapport-ETV-feb-2016.pdf.

22 K. Kohansal, K. Sharma, S. S. Toor, E. L. Sanchez and J. Zimmermann, Bio-Crude Production Improvement during Hydrothermal Liquefaction of Biopulp by Simultaneous Application of Alkali Catalysts and Aqueous Phase Recirculation, *Energies*, 2021, DOI: 10.3390/en14154492.

23 J. Watson, J. Lu, R. de Souza, B. Si, Y. Zhang and Z. Liu, Effects of the extraction solvents in hydrothermal liquefaction processes: Biocrude oil quality and energy conversion efficiency, *Energy*, 2019, **167**, 189–197, DOI: 10.1016/j.energy.2018.11.003.

24 N. D. Denkov, K. G. Marinova and S. S. Tcholakova, Mechanistic understanding of the modes of action of foam control agents, *Adv. Colloid Interface Sci.*, 2014, **206**, 57–67, DOI: 10.1016/j.cis.2013.08.004.

25 P. Biller, B. K. Sharma, B. Kunwar and A. B. Ross, Hydroprocessing of bio-crude from continuous hydrothermal liquefaction of microalgae, *Fuel*, 2015, **159**, 197–205, https://www.sciencedirect.com/science/article/pii/S0016236115006572.

26 F. Conti, S. S. Toor, T. H. Pedersen, T. H. Seehar and A. H. Nielsen, Valorization of animal and human wastes through hydrothermal liquefaction for biocrude production and simultaneous recovery of nutrients, *Energy Convers. Manage.*, 2020, **216**(February), 112925, DOI: **10.1016/j.enconman.2020.112925**.

27 C. Xu and T. Etcheverry, Hydro-liquefaction of woody biomass in sub- and super-critical ethanol with iron-based catalysts, *Fuel*, 2008, **87**(3), 335–345, **https://www.sciencedirect.com/science/article/pii/S0016236107002268**.

28 S. A. Channiwala and P. P. Parikh, A unified correlation for estimating HHV of solid, liquid and gaseous fuels, *Fuel*, 2002, **81**(8), 1051–1063, **https://www.sciencedirect.com/science/article/pii/S0016236101001314**.

29 S. Chiaberge, I. Leonardis, T. Fiorani, G. Bianchi, P. Cesti, A. Bosetti, *et al.*, Amides in Bio-oil by Hydrothermal Liquefaction of Organic Wastes: A Mass Spectrometric Study of the Thermochemical Reaction Products of Binary Mixtures of Amino Acids and Fatty Acids, *Energy Fuels*, 2013, **27**(9), 5287–5297, DOI: **10.1021/ef4009983**.

30 H. Li, H. Guo, Z. Fang, T. Aida and R. Smith, Cycloamination strategies for renewable N-heterocycles, *Green Chem.*, 2020, **22**, 582–611.

31 R. M. Lanigan and T. D. Sheppard, Recent developments in amide synthesis: Direct amidation of carboxylic acids and transamidation reactions, *Eur. J. Org. Chem.*, 2013, **33**, 7453–7465.

32 W. Abdelmoez, T. Nakahasi and H. Yoshida, Amino Acid Transformation and Decomposition in Saturated Subcritical Water Conditions, *Ind. Eng. Chem. Res.*, 2007, **46**(16), 5286–5294, DOI: **10.1021/ie070151b**.

33 R. B. Madsen, R. Z. K. Bernberg, P. Biller, J. Becker, B. B. Iversen and M. Glasius, Hydrothermal co-liquefaction of biomasses – quantitative analysis of bio-crude and aqueous phase composition, *Sustainable Energy Fuels*, 2017, **1**(4), 789–805, DOI: **10.1039/C7SE00104E**.

34 B. Maddi, E. Panisko, T. Wietsma, T. Lemmon, M. Swita, K. Albrecht, *et al.*, Quantitative characterization of the aqueous fraction from hydrothermal liquefaction of algae, *Biomass Bioenergy*, 2016, **93**, 122–130, **https://www.sciencedirect.com/science/article/pii/S0961953416302458**.

35 K. M. Isa, T. A. T. Abdullah and U. F. M. Ali, Hydrogen donor solvents in liquefaction of biomass: a review, *Renewable Sustainable Energy Rev.*, 2018, **81**, 1259–1268, **https://www.sciencedirect.com/science/article/pii/S1364032117305087**.

36 J. Lu, J. Zhang, Z. Zhu, Y. Zhang, Y. Zhao, R. Li, *et al.*, Simultaneous production of biocrude oil and recovery of nutrients and metals from human feces via hydrothermal liquefaction, *Energy Convers. Manage.*, 2017, **134**, 340–346, DOI: **10.1016/j.enconman.2016.12.052**.

37 A. Rezagama, M. Hibbaan and M. Arief Budihardjo, Ammonia-Nitrogen (NH 3-N) and Ammonium-Nitrogen (NH 4 +-N) Equilibrium on The Process of Removing Nitrogen By Using Tubular Plastic Media, *J. Mater. Environ. Sci.*, 2017, **8**(S), 4915–4922.

38 M. Déniel, G. Haarlemmer, A. Roubaud, E. Weiss-Hortala and J. Fages, Hydrothermal liquefaction of blackcurrant pomace and model molecules: understanding of reaction mechanisms, *Sustainable Energy Fuels*, 2017, **1**(3), 555–582.

39 P. Biller, R. B. Madsen, M. Klemmer, J. Becker, B. B. Iversen and M. Glasius, Effect of hydrothermal liquefaction aqueous phase recycling on bio-crude yields and composition, *Bioresour. Technol.*, 2016, **220**, 190–199, DOI: **10.1016/j.biortech.2016.08.053**.

40 X. Zhuang, J. Liu, C. Wang, Q. Zhang and L. Ma, A review on the stepwise processes of hydrothermal liquefaction (HTL): recovery of nitrogen sources and upgrading of biocrude, *Fuel*, 2021, (September), 122671.

41 L. Luo, J. D. Sheehan, L. Dai and P. E. Savage, Products and Kinetics for Isothermal Hydrothermal Liquefaction of Soy Protein Concentrate, *ACS Sustainable Chem. Eng.*, 2016, **4**(5), 2725–2733.

42 B. Motavaf and P. E. Savage, Effect of Process Variables on Food Waste Valorization via Hydrothermal Liquefaction, *ACS ES&T Engg*, 2021, **1**(3), 363–374.

43 I. Kristianto, B. S. Haynes and A. Montoya, Hydrothermal Decomposition of Glucose in the Presence of Ammonium, *Ind. Eng. Chem. Res.*, 2021, **60**(28), 10129–10138.

44 A. A. Shah, S. S. Toor, T. H. Seehar, K. K. Sadetmahaleh, T. H. Pedersen, A. H. Nielsen, *et al.*, Bio-crude production through co-hydrothermal processing of swine manure with sewage sludge to enhance pumpability, *Fuel*, 2021, **288**, 119407, **https://www.sciencedirect.com/science/article/pii/S0016236120324030**.

45 G. Goswami, B. B. Makut and D. Das, Sustainable production of bio-crude oil via hydrothermal liquefaction of symbiotically grown biomass of microalgae-bacteria coupled with effective wastewater treatment, *Sci. Rep.*, 2019, **9**(1), 1–12, DOI: **10.1038/s41598-019-51315-5**.

46 E. A. Ramos-Tercero, A. Bertucco and D. W. F. Brilman, Process water recycle in hydrothermal liquefaction of microalgae to enhance bio-oil yield, *Energy Fuels*, 2015, **29**(4), 2422–2430.

47 J. Ancheyta, G. Marroquín, M. J. Angeles, M. J. Macías, I. Pitault, M. Forissier, *et al.*, Some experimental observations of mass transfer limitations in a trickle-bed hydrotreating pilot reactor, *Energy Fuels*, 2002, **16**(5), 1059–1067.

48 J. A. Melero, J. Iglesias, G. Morales and M. Paniagua, *13 – Chemical routes for the conversion of cellulosic platform molecules into high-energy-density biofuels*, ed. R. Luque, C. S. K. Lin and K. Wilson, Clark JBT-H of BP, Woodhead Publishing, 2nd edn, 2016, pp. 359–88, **https://www.sciencedirect.com/science/article/pii/B9780081004555000138**.

49 M. S. Haider, D. Castello and L. A. Rosendahl, The Art of Smooth Continuous Hydroprocessing of Biocrudes Obtained from Hydrothermal Liquefaction: Hydrodemetallization and Propensity for Coke Formation, *Energy Fuels*, 2021, **35**(13), 10611–10622.

50 M. Déniel, G. Haarlemmer, A. Roubaud, E. Weiss-Hortala and J. Fages, Bio-oil Production from Food Processing Residues: Improving the Bio-oil Yield and Quality by Aqueous Phase Recycle in Hydrothermal Liquefaction of Blackcurrant (Ribes nigrum L.) Pomace, *Energy Fuels*, 2016, **30**(6), 4895–4904, DOI: **10.1021/acs.energyfuels.6b00441**.

51 A. Srifa, K. Faungnawakij, V. Itthibenchapong, N. Viriya-empikul, T. Charinpanitkul and S. Assabumrungrat, Production of bio-hydrogenated diesel by catalytic hydrotreating of palm oil over NiMoS2/γ-Al2O3 catalyst, *Bioresour. Technol.*, 2014, **158**, 81–90, **https://www.sciencedirect.com/science/article/pii/S0960852414001254**.

52 M. J. Girgis, B. C. Gates and M. J. Girgis, Reactivities, Reaction Networks, and Kinetics in High-Pressure Catalytic Hydroprocessing, *Ind. Eng. Chem. Res.*, 1991, **30**(9), 2021–2058.

53 J. R. Katzer and R. Sivasubramanian, Process and Catalyst Needs for Hydrodenitrogenation, *Catal. Rev.*, 1979, **20**(2), 155–208.

54 N. Sudasinghe, J. R. Cort, R. Hallen, M. Olarte, A. Schmidt and T. Schaub, Hydrothermal liquefaction oil and hydrotreated product from pine feedstock characterized by heteronuclear two-dimensional NMR spectroscopy and FT-ICR mass spectrometry, *Fuel*, 2014, **137**, 60–69, **https://www.sciencedirect.com/science/article/pii/S0016236114007200**.

55 H. Wu, H. Li and Z. Fang, Hydrothermal amination of biomass to nitrogenous chemicals, *Green Chem.*, 2021, **23**(18), 6675–6697.

56 C. U. Jensen, J. Hoffmann and L. A. Rosendahl, Co-processing potential of HTL bio-crude at petroleum refineries. Part 2: A parametric hydrotreating study, *Fuel*, 2016, **165**, 536–543, **https://www.sciencedirect.com/science/article/pii/S001623611500856X**.

57 G. D. Strahan, C. A. Mullen and A. A. Boateng, Characterizing biomass fast pyrolysis oils by 13C NMR and chemometric analysis, *Energy Fuels*, 2011, **25**(11), 5452–5461.

